Slow waves, surface waves and their applications

Keith Attenborough, Imran Bashir, Ho-Chul Shin, Shahram Taherzadeh

ACOUSTICS 2012

Slow waves, surface waves and their applications

K. Attenborough, I. Bashir, H.-C. Shin and S. Taherzadeh

The Open University, DDEM, Maths, Computing and Technology, Walton Hall, MK7 6AA
Milton Keynes, UK
k.attenborough@open.ac.uk

Fluid-saturated porous elastic solids support two compressional wave types, often called 'fast' and 'slow', and a shear wave. Walter Lauriks recognised the commonality of the physical mechanisms which govern the acoustical properties of such media and initiated a great many studies ranging from the acoustical monitoring of marrow filled bone to properties of air-filled bread, soils and snow. The Biot parameter values that create distinct slow waves in transmission experiments are explored. There are two types of surface waves at a poroelastic boundary: a fluid-coupled Rayleigh wave and a wave that depends on the surface impedance. A rough hard surface is also able to generate an acoustic surface wave. Walter Lauriks studied pore-related surface waves and those over a periodically-rough hard surfaces. It is shown that propagation over hard-backed square lattice grating layers modelled previously using modal analysis can be described as that over a square pore layer. Similarly propagation over rectangular grooves or bosses also modelled previously using modal analysis can be modelled as that over a slit pore layer.

1 Introduction

Many of the predictions used when studying fluid-saturated porous media with elastic frames, i.e. poroelastic media, are based on Biot theory [1]. The theory assumes that the incident wavelengths are much larger than the constituent solid particles and pores, i.e. $\lambda >> a$ where λ represents the wavelength and a represents a characteristic microstructural dimension. An important prediction of the theory is that, as well as a shear wave, there are two kinds of compressional waves: a Type 1 'fast' wave which travels predominantly in the solid frame and a Type 2 'slow' or fluid borne wave which travels mainly in the pore fluid. The 'fast' wave involves coupled motion in which fluid and solid frame move together and the 'slow' wave involves motion in which fluid and frame are moving out of phase i.e. are essentially decoupled.

There is a long and continuing history of skepticism in the underwater acoustics community about the existence of the 'slow' wave [2]. Partly this stems from the inability of the original Biot theory to explain the observed frequency dependence of attenuation in underwater sediments. In its original form Biot theory predicts that fast wave attenuation is proportional to f^2 (where f represents frequency) at low frequencies and $\sqrt{f}$ at high frequencies. Several sets of data suggest a more or less linear dependence over a wide frequency range. In classical experiments on water-filled glass beads, the slow wave was measurable only when the beads were fused together. The non-appearance of the slow wave when the beads were unconsolidated has been attributed to the 'weak' frame [3]. However it seems that other important factors were the saturation with water and the method of excitation used since 'slow' waves have been observed in air-filled unconsolidated glass beads and sand subject to acoustical (non-contact) excitation [4].

The 'slow' wave is the dominant type of wave in air-filled porous media with relatively stiff frames [5]. There have been many studies of the influence of the porous structure on the acoustical properties of such media and additional parameters have been introduced to allow for arbitrary pore structure [6]. The conditions for observing separate 'fast' and 'slow' waves in measurements of pulse transmission through fluid-saturated poroelastic layers and the issue of the frequency-dependence of the 'fast' wave in water-saturated sediments are discussed in section 2.

Two types of surface wave result from excitation from a point source located above air-filled porous elastic media. One of these surface waves depends primarily on the properties of the solid frame and is similar to the Rayleigh wave observed at the free boundary of an elastic solid [7] travels at a little less than the speed of sound in air. The other type of surface wave is related primarily to the pore structure in that it is the only such wave that is observed above a rigid-framed porous layer.

Classical studies of the surface waves induced by long wavelength coherent scattering from a rough surface have been made by Tolstoy [8] and Lucas and Twersky [9]. The latter work considers periodic as well as random roughness. A particular example of a periodically-rough surface is the square lattice surface formed by a double layer of commercial overhead lighting panels. A comb-like surface is expected to be locally-reacting and to have purely imaginary normalised impedance given by

$$Z(L)/\rho c = \coth(-ikL). \quad (1)$$

where L is the (double) layer thickness and $k = \omega/c$ is the wave number in air. However it has been found that (a) the lattice surface is not locally-reacting and (b) the angle-dependent impedance has a non-zero resistive component. This has been explained in terms of leakage between the stacked layers. An exact analytical solution has been obtained for plane wave scattering by a lattice surface consisting of square cells of side a and depth L having infinitely thin walls and assuming leakage between the cell partitions [10]. A distinction has been drawn between surface wave and diffraction modes. The grating is found to be equivalent to an impedance plane at low frequencies when only a specularly-reflected wave exists and to be locally-reacting if $L/a >> 1$ and $\lambda/a >> 1$. As well as surface wave creation at low frequencies for incident curved wave fronts, at high frequencies such that wavelengths are comparable to the grating period, the possibility of generating large amplitude surface waves over a grating in either the backward or forward directions with homogeneous plane-waves has been predicted. Surface waves over rectangular grooves and lattice layers have been analysed using a modal theory deduced from studies of electromagnetic wave propagation [11,12]. The analysis was carried out ignoring viscous and thermal effects. Modal analysis predicts a reduced effective layer depth and provides good agreement with surface wave data.

Propagation over rectangular grooves in an acoustically-hard surface should be equivalent to that over a hard-backed rigid-framed layer containing slit-like pores [1,13]. Similarly propagation over a square lattice layer should be equivalent to that over a rigid-porous layer containing square pores [14]. These equivalencies are explored in respect of excess attenuation spectra due to a point source and deduced surface impedance in section 3. Measurements and predictions of surface wave dispersion, excess attenuation and impedance spectra are reported. It is found that viscous friction effects are not negligible. Concluding remarks are made in section 4.

2 Slow and fast wave transmission

2.1 Pulse separation

The arrival of two distinct compressional waves has been observed frequently in measurements of ultrasonic pulse transmission through water-filled bone samples [see for example ref.15]. It has proved more difficult to observe separate arrivals in pulse transmission through water-filled sediments [16]. Figures 1 and 2 compare the dispersion and attenuation spectra predicted using Biot theory with the representative parameter values of water-filled bone and sand listed in Table 1. Viscous and thermal effects have been predicted by assuming identical slit-pores rather than, for example, by using the Johnson-Allard model [15]. More sophisticated models of these effects require additional parameters; values of which have been determined mainly for air-filled absorbing materials but are not extensively available for other media. The parallel slit idealisation of the pore structure does not have a large influence on the conclusions that can be reached concerning the comparative properties of 'fast' and 'slow' waves.

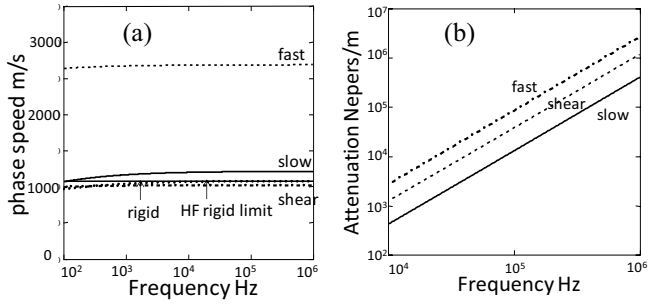

Figure 1: Predictions of (a) dispersion and (b) attenuation spectra for compressional and shear waves in **water-filled bone** characterised by the parameters listed in Table 1. The dispersion predictions include high-frequency and rigid-frame limits for the slow wave.

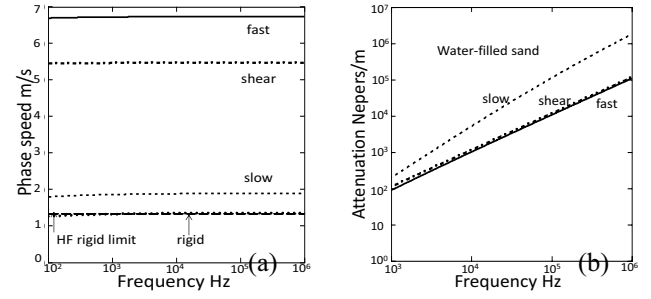

Figure 2: Predictions of (a) dispersion and (b) attenuation spectra for compressional and shear waves in **water-filled sand** characterized by the parameters listed in Table 1. The dispersion predictions include high-frequency and rigid-frame limits for the 'slow' wave.

Although the predicted 'fast' and 'slow' wave speeds are sufficiently different in both water-filled media that, in principle, they should separate during transmission through a thick sample, in the water-filled sand the attenuation of the 'slow' wave is significantly higher than that of the fast wave and increases much more rapidly with increasing frequency. This makes 'slow' wave observation difficult.

Separate arrivals of 'fast' and 'slow' waves have been found in transmission through a 5 cm thick layer of partially-reticulated polyurethane foam [17]. The parameters deduced by fitting these data indicate a relatively high tortuosity value (7.8) for this foam. This ensures that the 'slow' wave is significantly 'slow'. Together with the relatively high bulk modulus (1700 kPa) of this foam, the high tortuosity ensures that the 'slow' wave speed is substantially lower than that of the 'fast' wave thereby giving a substantial time delay between the two wave types during transmission through the 5 cm layer.

Table 1 Parameter values used for the predictions in Figures 1-3

Parameter	Water-filled cancellous bone	Water-filled sand	Air-filled partially-reticulated foam [18]
Density of solid, ρ_s kg/m^3	1960	2650	1200
Density of fluid, ρ_f, kg/m^3	1000	1000	1.2
Fluid specific heat ratio, γ	1.0107	1.0107	1.4
Prandtl number, N_{PR}	7		0.71
Porosity, Ω	0.65	0.3	0.98
Flow resistivity Pa s m^{-2}	200	10000	8760
Tortuosity	1.9	1.25	2.19
Bulk modulus of solid K_s GPa	20	20	0.0625
Bulk modulus of solid frame, K_b GPa	4.7	2.25	6.89×10^{-4}
Bulk loss factor	0	0.02	0.09
Rigidity Modulus of solid frame, GPa	1.035	0.13	1.15×10^{-5}
Rigidity loss factor	0	0.02	0.09
(Adiabatic) Bulk modulus of fluid, K_f GPa	2.2		1.4×10^{-4}

Wave speeds have been obtained from transmission measurements on a layer of polyurethane foam subjected to mechanical and acoustical excitation. The acoustical excitation was provided by a point source loudspeaker and the point mechanical excitation was through a rod and plate attached to a shaker. The acoustical transmission was monitored by a microphone and the frame disturbance on both sides was monitored by a Laser-Doppler vibrometer. The measurement methods and parameter deduction methods are described more fully elsewhere [18]. Fig. 3(a) compares resulting data with predictions based on the parameter values listed in Table 1. The speeds deduced from the receiving microphone are represented by asterisks and those deduced from frame displacements are represented by filled circles. These data and predictions are consistent with 'switching' between Type 1 and Type 2 waves near 1 kHz. As indicated by the prediction for a rigid frame, the frame displacement arrivals are effectively those for the 'slow' wave below 1 kHz and those for the 'fast wave above 1 kHz. Similarly the speeds deduced from acoustical excitation correspond to 'fast' wave arrivals below 1 kHz and 'slow' wave arrivals above 1 kHz. The

predicted fluid-to-solid amplitude ratios in Figure 3(b) also show that below 1 kHz the largest fluid amplitudes are associated with the Type 1 wave and above 1 kHz with the Type 2 wave: these latter amplitudes are negative since the fluid and solid motions are out of phase. The shear wave is predicted to involve relatively little fluid motion.

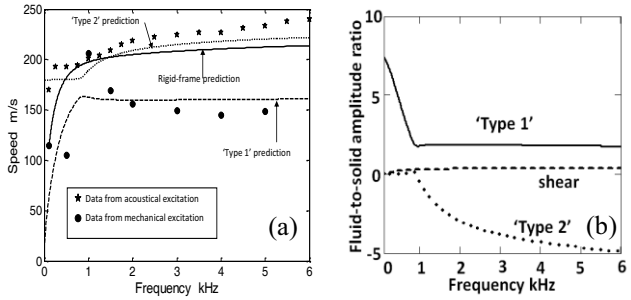

Figure 3: (a) Measured dispersion (points) of two compressional waves in an **air-filled foam** compared with predictions (dashed lines and dots) using the parameters listed in Table 1 deduced by fitting acoustic-to-frame coupling data [18]; also shown is the rigid frame limit (continuous line) (b) predicted frequency dependence of the ratios of fluid to solid particle displacement amplitudes for each of the two compressional waves.

2.2 Fast wave attenuation spectra

Figure 4 shows that without including any frame losses Biot theory predicts a fast wave attenuation spectrum in water-filled sand that is close to $f^{3/2}$ dependence between 1 and 6 kHz. However the inclusion of frame losses (see table 1) alters the frequency dependence to one that is near linear. Use of complex elastic moduli is standard in Biot-Stoll theory [19]. However, as demonstrated in Fig.4, inclusion of a pore size distribution, even without using complex elastic moduli, also alters the predicted frequency dependence to be near linear over part of the frequency range of interest.

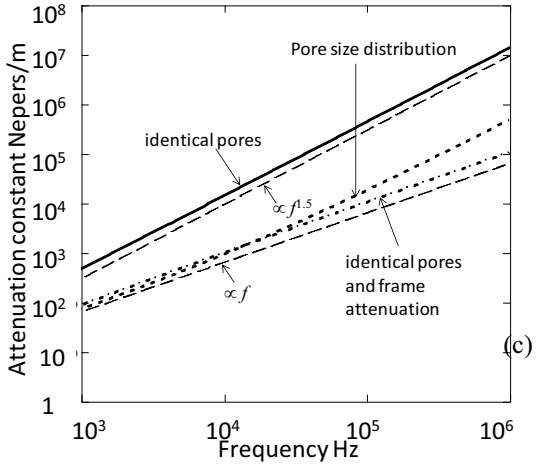

Figure 4: Predicted attenuation spectra in a water filled sand (Table 1) without frame losses and identical pores (solid line), a pore size distribution (heavy broken line) and with identical and pores frame losses (dash-dot line).

The predictions for a pore size distribution have been obtained by using a two-parameter Padé approximation corresponding to a log-normal distribution of pore sizes with standard deviation of 2 phi units [13,20].

3 Excess attenuation and deduced impedance spectra over square cell lattice layers

3.1 Excess Attenuation

Figure 5 shows the arrangement used to measure propagation over the surfaces of single, double and triple square cell lattice layers each of depth 0.0126 m. The cell width is 0.014 m and cell wall thickness is 0.00014 m. The corresponding porosity is 0.98. The flow resistivity, R_s, of a medium of porosity Ω containing square pores of side a saturated by a fluid with coefficient of fluid viscosity μ is given by

$$R_s = 28.48\mu/\Omega a^2, \tag{2}$$

Using the known dimensions of the lattice cells and cell walls, Eq.(2) gives a flow resistivity of 2.7 Pa s m^{-2}. The neglect of viscous and thermal effects when predicting the acoustical properties of the lattice with cell dimension 0.014 m using modal analysis [11] is reasonable since the cell dimension is much larger than the viscous or thermal boundary layer thickness and is consistent with the rather low value of flow resistivity.

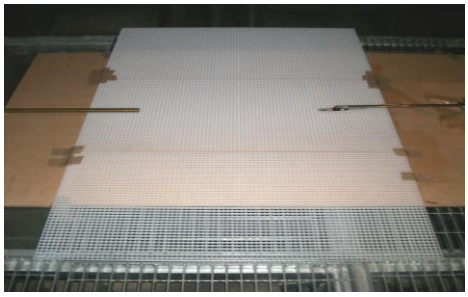

Figure 5: Measurement of propagation over lattice layers.

According to modal analysis [11], if viscous losses are neglected and the squares in the lattice have depth L, side a and wall thickness $(d - a)$, then, at wavelengths larger than a, the normalised impedance model for the hard-backed lattice is given by

$$Z(L)/\rho c = (1/\Omega)\coth(-ikL'), \tag{3}$$

where $\Omega = (a/d)^2$ and effective depth $L' = (L - a\log(2)/\pi)$.

The surface impedance of a hard-backed layer of rigid material of thickness L, containing square pores is given by [13,14]

$$Z(L) = Z_c \coth(-ikL), \tag{4}$$

$$Z_c(\omega) = (\rho_f c_f)^{-1}[(1/\Omega^2)\rho(\omega)/C(\omega)]^{0.5}, \tag{5}$$

$$k(\omega) = \omega[(\rho(\omega)C(\omega)]^{0.5}, \tag{6}$$

$$\rho(\omega) = \rho_0/\mathrm{H}(\lambda),\ C(\omega) = (\gamma P_0)^{-1}[\gamma - (\gamma - 1)\mathrm{H}(\lambda\sqrt{(N_{PR})})] \tag{7}$$

$$\mathrm{H}(\lambda) = \frac{4}{\pi^4}\Sigma\{(m+0.5)^2(n+0.5)^2[1+2i((m+0.5)^2+(n+0.5)^2)/\lambda^2]\}^{-1} \tag{8}$$

where $\lambda = (a/\pi)\sqrt{(2\omega\rho/\mu)}$, ω is the angular frequency, ρ is the fluid density and the (infinite) summation in Eq.(7) is over the modal indices (m,n).

Details of methods of calculating EA spectra for a given surface impedance and source-receiver geometry may be found elsewhere [13]. Figure 6 shows predictions of excess attenuation (EA) spectra over a single lattice layer with source and receiver at 0.05 m height above the acoustically-hard base and separated by 0.7 m. The predictions have been made assuming that the lattice layer is locally-reacting and using (i) Eq. (2), (ii) slit-like pores [13] and (iii) square pores (Eqs. (3) - (7)) with the known lattice porosity and flow resistivity. These predictions are practically identical.

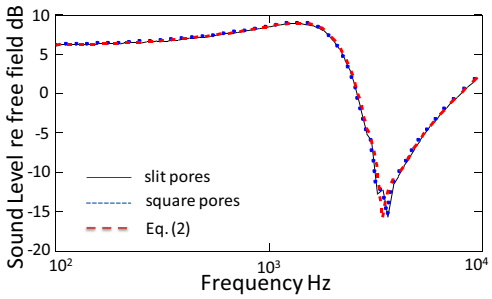

Figure 6: Predicted excess attenuation spectra with source and receiver heights of 0.05 m and separation 0.7 m over a single square cell lattice layer using an effective layer depth of 0.011 m and three impedance models (see text).

Figures 7(a)–(c) compare measurements and predictions of Excess Attenuation (EA) spectra over single, double and triple lattice layers respectively with (point) source and receiver at a height of 0.05 m above the lattice and separated by 0.7 m. The predictions use the surface impedance calculated from Eqs. (3) – (7) with m = n = 500 and an effective layer depth $L' = (L - a\log(2)/\pi)$. There is reasonable agreement between predictions and data.

3.2 Deduced impedance and surface wave dispersion

Complex attenuation data may be used to deduce surface impedance as long as the surface is locally reacting [21]. Figure 8 compares impedance spectra deduced in this manner for a triple lattice layer with those predicted by the slit pore model (continuous real, broken imaginary lines) using the measured depth (0.038 m) and Eq. (3) with an effective depth (0.036 m). Again there is not much difference between the predictions but neither of the predictions agrees well with the deduced impedance spectra. Eq. (3) predicts purely imaginary surface impedance (continuous black line) whereas the slit pore model predicts a non-zero real part which is evident also in the deduced impedance. A phase gradient method has been used to measure the surface wave dispersion. Example data and predictions for the triple lattice layer are shown in Fig. 9. The deduced impedance gives best agreement with data.

4 Conclusion

Biot theory, modified by Allard and others, is a powerful tool for understanding and exploiting the acoustical properties of poroelastic media. In particular the 'slow' wave is an important contributor to the acoustical properties of air-filled media and to transmission through water-filled bone. It is harder to observe in water-filled sediments. An application of Biot theory to remote monitoring of unsaturated soil conditions is reported elsewhere [22].

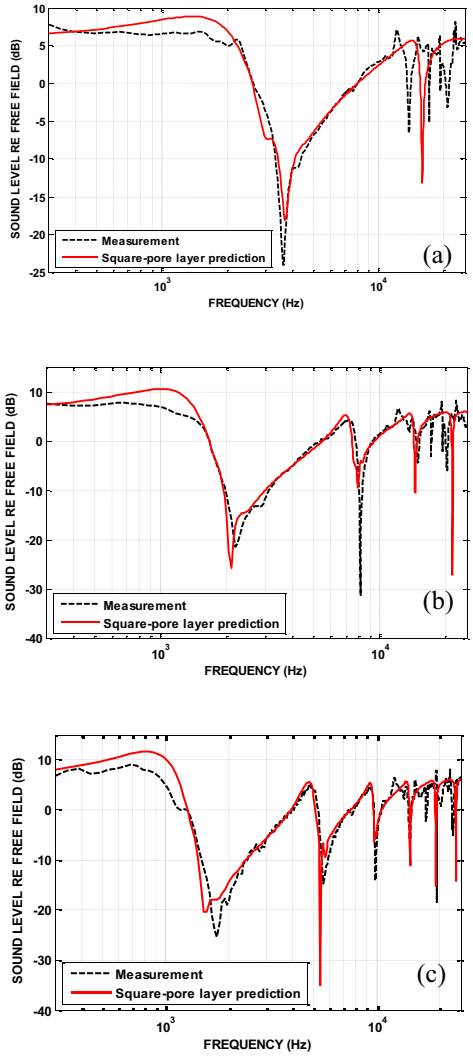

Figure 7: Measured and predicted excess attenuation spectra with source and receiver height of 0.05 m and separation 0.7 m over (a) a single square lattice layer, effective layer depth 0.011 m. (b) double lattice layer, effective layer depth 0.024 m (c) triple lattice layer, effective layer depth 0.036 m.

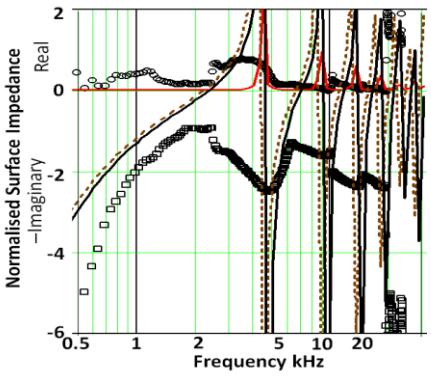

Figure 8: Deduced (points) and predicted impedance spectra for a triple lattice layer, effective layer depth 0.036 m. (key in text).

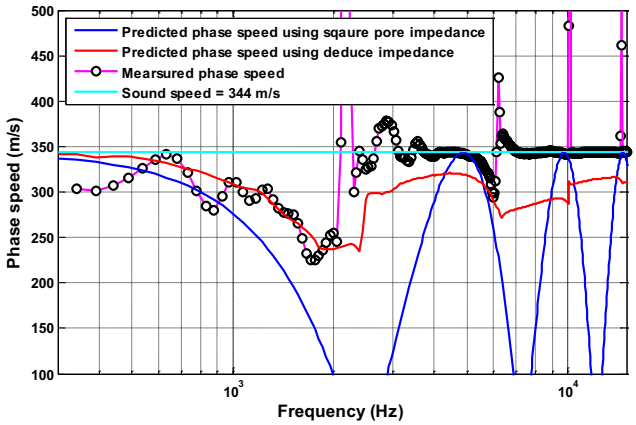

Figure 9: Measured surface wave dispersion (joined circles) over a triple lattice layer and predictions using the square pore impedance model (Eqs. (3) - (7) blue line) or the impedance deduced from complex excess attenuation data (red line).

Surface waves travelling at slightly less than the speed of sound in air are common to sound propagation near grazing over porous layers and randomly- or periodically-rough boundaries. The propagation of sound over periodically rough surfaces is of interest in designing ground effects for noise control.

Acknowledgments

The research leading to these results has received funding from the European Community's Seventh Framework Programme (FP7/2007-2013) under grant agreement n° 234306, collaborative project HOSANNA, and from EPSRC (UK) grant EP/H040617/1.

References

[1] M. A. Biot, "Theory of propagation of elastic waves in a fluid-saturated porous solid, I. Low-frequency range, II. Higher frequency range", J. Acoust. Soc. Am. **28**, 168 – 178, 179 – 191 (1956)

[2] A. D. Pierce and W. M. Carey, "Critique of Biot-related theories of acoustic waves in porous media" Proc. ICA Sydney 23 – 27 August 2010

[3] D. L. Johnson and T. J. Plona, "Acoustic slow waves and the consolidation transition", J. Acoust. Soc. Am. **72** (2) 556 – 565 (1982)

[4] C. K. Frederickson, J. M. Sabatier and R. Raspet, "Acoustic characterization of rigid-frame air-filled porous media using both reflection and transmission measurements", J. Acoust. Soc. Am. **99** (3) 1326 – 1332 (1996)

[5] K. Attenborough, "Acoustical characteristics of rigid fibrous absorbents and granular materials", J. Acoust. Soc. Am. **73**(3) 785-799, (1983)

[6] J. F. Allard and N. Atalla, *Propagation of sound in porous media*, John Wiley & Sons (2009)

[7] K. Attenborough and T. L. Richards "Solid particle motion induced by a point source above a poroelastic half-space" J. Acoust. Soc. Am. **86** 1085 – 1092 (1989)

[8] I. Tolstoy, "Smoothed boundary conditions, coherent low-frequency scatter, and boundary modes" J. Acoust. Soc. Am. **75**, 1-22 (1984)

[9] R. J. Lucas and V. Twersky, "Coherent response to a point source irradiating a rough plane" J. Acoust. Soc. Am. **76**, 1847 – 1863 (1984)

[10] W. Zhu, M. R. Stinson and G. A. Daigle, "Scattering from impedance gratings and surface wave formation", J. Acoust. Soc. Am. **111** 1996 – 2012 (2002)

[11] L. Kelders, J. F. Allard and W. Lauriks, "Ultrasonic surface waves above rectangular-groove gratings", J. Acoust. Soc. Am. **103** 2730 – 2733 (1998)

[12] J. F. Allard, L. Kelders and W. Lauriks, "Ultrasonic surface waves above a doubly periodic grating", J. Acoust. Soc. Am. **105** 2528 – 2531 (1999)

[13] K. Attenborough, K. M. Li and K. Horoshenkov, *Predicting Outdoor Sound*, Taylor and Francis, (2006).

[14] H.-S. Roh, W. P. Arnott, J. M. Sabatier and R. Raspet, "Measurement and calculation of acoustic propagation constants in arrays of small air-filled rectangular tubes" J. Acoust. Soc. Am. **89** 2617 – 2624 (1991)

[15] Z. E. A. Fellah, J. Y. Chapelon, S. Berger, W. Lauriks and C. Depollier, "Ultrasonic wave propagation in human cancellous bone: Application of Biot theory", J. Acoust. Soc. Am. **116** 61 – 73 (2004)

[16] D. M. J. Smeulders, "Experimental evidence for slow compressional waves", J. Eng. Mech. ASCE 908 – 917 (2005)

[17] J. S. Bolton and E. R. Green, "Normal Incidence Sound Transmission through Double-Panel Systems Lined with Relatively Stiff, Partially Reticulated Polyurethane Foam", Applied Acoustics **39** 23 – 51 (1993)

[18] H.-C. Shin, S. Taherzadeh and K. Attenborough, "Estimation of acoustic and elastic properties of plastic foam using acoustic-to-frame coupling", Acoustics 2012 Nantes, paper 201 PU-S02

[19] R. D. Stoll, "Acoustic waves in saturated sediments", In: *Physics of sound in marine sediments* (ed: L. Hampton), Plenum Press, New York (1974)

[20] K. V. Horoshenkov, K. Attenborough, S.N. Chandler-Wilde, "Pade approximants for the acoustical properties of rigid frame porous media with pore size distribution", J. Acoust. Soc. Am. **104**, 1198 – 1209 (1998)

[21] S. Taherzadeh and K. Attenborough "Deduction of ground impedance from measurements of excess attenuation spectra" J. Acoust. Soc. Am. **105** (3) 2039-2042 (1999)

[22] H.-C. Shin, S. Taherzadeh, K. Attenborough and R. Whalley, "Use of short range outdoor sound propagation and acoustic-to- seismic coupling to deduce soil state", Acoustics 2012 Nantes, paper 201 EN-S01